

**MATHEMATICAL ENGINEERING
TECHNICAL REPORTS**

**MIMO Zero-Forcing Detection Performance
Evaluation by Holonomic Gradient Method**

Constantin SIRITEANU, Akimichi TAKEMURA and
Satoshi KURIKI

METR 2014-08

March 2014

DEPARTMENT OF MATHEMATICAL INFORMATICS
GRADUATE SCHOOL OF INFORMATION SCIENCE AND TECHNOLOGY
THE UNIVERSITY OF TOKYO
BUNKYO-KU, TOKYO 113-8656, JAPAN

WWW page: <http://www.keisu.t.u-tokyo.ac.jp/research/techrep/index.html>

The METR technical reports are published as a means to ensure timely dissemination of scholarly and technical work on a non-commercial basis. Copyright and all rights therein are maintained by the authors or by other copyright holders, notwithstanding that they have offered their works here electronically. It is understood that all persons copying this information will adhere to the terms and constraints invoked by each author's copyright. These works may not be reposted without the explicit permission of the copyright holder.

MIMO Zero-Forcing Detection Performance Evaluation by Holonomic Gradient Method

Constantin Siriteanu, Akimichi Takemura, Satoshi Kuriki

Abstract

We have recently derived *infinite-series expressions* for performance measures of multiple-input multiple-output (MIMO) spatial multiplexing with zero-forcing detection (ZF) for Rician–Rayleigh fading, which is relevant in heterogeneous networks. These *expressions* ensue from a well-known infinite-series expansion around $\sigma = 0$ of the confluent hypergeometric function ${}_1F_1(\cdot, \cdot, \sigma)$. Theoretically, this expansion converges for any σ . Numerically, convergence becomes slow with increasing σ . Consequently, our ZF performance-measure expressions diverge numerically at practically-relevant Rician K -factor values. Therefore, herein, we deploy instead the *holonomic gradient method* (HGM), which computes a function by numerically solving the differential equation it satisfies. HGM is applicable because ${}_1F_1(\cdot, \cdot, \sigma)$ is *holonomic*, i.e., it satisfies a differential equation with polynomial coefficients with respect to σ . First, using properties of holonomic functions, we reveal that the moment generating function (m.g.f.) and probability density function (p.d.f.) of the ZF signal-to-noise ratio (SNR) are holonomic. Then, from the differential equation for ${}_1F_1(\cdot, \cdot, \sigma)$, we deduce those satisfied by the SNR m.g.f. and p.d.f. HGM is shown to yield accurate p.d.f. computation for practically-relevant values of K (at which infinite-series truncation breaks down). Numerical integration of the SNR p.d.f. obtained from HGM yields accurate outage probability and ergodic capacity assessments for MIMO ZF under Rician–Rayleigh fading.

Index Terms

Confluent hypergeometric function, differential equation, holonomic function, infinite-series, holonomic gradient method, MIMO, numerical convergence, Rayleigh and Rician (Ricean) fading, spatial multiplexing, zero-forcing.

I. INTRODUCTION

A. Background, Previous Work, and Motivation

The performance evaluation for multiple-input multiple-output (MIMO) wireless communications systems has attracted substantial interest over the past decade [1] [2] [3]. Typically, this evaluation proceeds from performance-measure (e.g., average error probability (AEP), outage probability, ergodic capacity) expressions derived based on statistical assumptions about the channel-fading matrix. However, MIMO analyses have often assumed zero-mean MIMO channel matrix, i.e., Rayleigh fading, for tractability, although state-of-the-art channel measurements and models, e.g., WINNER II [4], have revealed that, in practice, the mean is typically nonzero, i.e., the fading is Rician. MIMO performance analysis for Rician fading is complicated by the ensuing noncentral Wishart matrix distribution [5]. Then, even for linear, i.e., low-complexity, interference-mitigation approaches such as zero-forcing detection (ZF), the performance analysis of MIMO spatial-multiplexing is much less tractable than for Rayleigh fading [6]. Nonetheless, with the advent of the massive-MIMO concept, it is likely that low-complexity detection methods such as ZF shall remain practically relevant [7] [8].

Since ZF for MIMO Rician fading remains of interest, we have analyzed ZF recently in [6] [9] for Rician–Rayleigh fading, i.e., when the intended Stream 1 undergoes Rician fading, whereas the interfering streams undergo Rayleigh fading. This fading model is relevant in macrocells, microcells, and heterogeneous networks, as explained in [6], and allows for a tractable exact analysis of ZF. Thus,

C. Siriteanu and A. Takemura are with the Department of Mathematical Informatics, Graduate School of Information Science and Technology, University of Tokyo, Japan, and Japan Science and Technology Agency, CREST.

S. Kuriki is with the Institute of Statistical Mathematics, Tachikawa, Tokyo, Japan.

in [6] we derived infinite-series expressions for its performance measures, and in [9] we proved that they converge everywhere. However, we found that truncating the derived infinite series yields numerical convergence only for a limited range of values for the Rician K -factor that is also unrealistic, according to WINNER II.

The underlying reason for these numerical convergence difficulties is that the ZF performance-measure expressions have been deduced in [6] from the widely-used infinite-series expression [10, Eq. (13.2.2), p. 322] for the confluent hypergeometric function ${}_1F_1(\cdot, \cdot, \sigma)$, where σ is a scalar argument. The numerical-convergence difficulties of this series have been acknowledged and tackled in [11] and references therein. Their cause is that the infinite series is an expansion around $\sigma = 0$. Therefore, with increasing σ , the numerical convergence of truncating the infinite-series expression [10, Eq. (13.2.2), p. 322] is increasingly difficult and eventually fails [11].

An alternative approach to computing ${}_1F_1(\cdot, \cdot, \sigma)$ that is not frequently used is based on the fact that this function satisfies, with respect to (w.r.t.) σ , the linear differential equation with polynomial coefficients from [10, Eq. (13.2.1), p. 322], i.e., it is *holonomic* [12, p. 334] [13, p. 7] [14, p. 140] [15, Section 6.4]. Holonomic functions can be computed at some σ by numerically solving their differential equation starting from an initial σ_0 where 1) the function is known analytically, or 2) the function can be approximated accurately, e.g., ${}_1F_1(\cdot, \cdot, \sigma_0)$ from its infinite series, for $\sigma_0 \approx 0$. This approach is known as the *holonomic gradient method* (HGM) [16] [17]. It has recently been applied to evaluating the normalizing constant of the Bingham distribution [16] and the cumulative distribution function (c.d.f.) of the dominant eigenvalue of a Wishart-distributed matrix [17].

B. Approach and Contribution

This paper demonstrates that HGM can help accurately compute MIMO performance-measure expressions obtained in terms of the confluent hypergeometric function ${}_1F_1(\cdot, \cdot, \cdot)$, for practical fading-parameter values. We proceed as follows, for ZF under Rician-Rayleigh fading. We start with [6, Eq. (31)], which expresses the moment generating function (m.g.f.) of the signal-to-noise ratio (SNR) for Stream 1 in terms of ${}_1F_1(\cdot, \cdot, \sigma)$. Its infinite-series expansion around the origin yielded, after inverse-Laplace transformation, the infinite-series expression for the SNR probability density function (p.d.f.) from [6, Eq. (39)].

Herein, we exploit instead the differential equation [10, Eq. (13.2.1), p. 322] satisfied by ${}_1F_1(\cdot, \cdot, \sigma)$ and deduce the corresponding differential equation for the ZF SNR m.g.f. Inverse-Laplace transformation yields the differential equation satisfied by the ZF SNR p.d.f., which is then numerically computed with the HGM. This approach starts from an initial value computed by truncating the infinite-series p.d.f. expression [6, Eq. (39)]. Finally, numerical integration of the SNR p.d.f. output by the HGM yields accurately, for the first time, the ZF outage probability and ergodic capacity for K values relevant for WINNER II.

C. Paper Organization

Section II describes the MIMO signal, noise, and channel models. Section III introduces the SNR m.g.f. and p.d.f. infinite-series expressions derived in [6]. Section IV discusses difficulties encountered in the truncation-based computation of the infinite-series expression for ${}_1F_1(\cdot, \cdot, \sigma)$ and of the ensuing infinite-series expression for the ZF SNR p.d.f. Section V defines holonomic functions and deduces from their properties that the SNR m.g.f. and p.d.f. are holonomic. This justifies our search in Section VI for the differential equations they satisfy. These differential equations are exploited in the HGM to generate the numerical results shown and discussed in Section VII. Finally, Section VIII discusses other possible HGM applications in MIMO evaluation. Throughout this paper we employ the same notation as in [6].

II. SIGNAL, NOISE, AND FADING MODELS [6]

Herein, the signal, noise, and channel models and assumptions follow closely the ones from [6]. Thus, we consider uncoded MIMO spatial-multiplexing over a frequency-flat fading channel. We assume that

there are N_T and N_R antenna elements at the transmitter(s) and receiver, respectively, with $N_T \leq N_R$, and denote the number of degrees of freedom as

$$N = N_R - N_T + 1. \quad (1)$$

Letting $\mathbf{x} = [x_1 x_2 \cdots x_{N_T}]^T$ denote the $N_T \times 1$ zero-mean transmit-symbol vector with $\mathbb{E}\{\mathbf{x}\mathbf{x}^H\} = \mathbf{I}_{N_T}$, the $N_R \times 1$ vector with the received signals can be represented as [1, Eq. (8)] [6, Eq. (1)]:

$$\mathbf{r} = \sqrt{\frac{E_s}{N_T}} \mathbf{H}\mathbf{x} + \mathbf{v} = \sqrt{\frac{E_s}{N_T}} \mathbf{h}_1 x_1 + \sqrt{\frac{E_s}{N_T}} \sum_{k=2}^{N_T} \mathbf{h}_k x_k + \mathbf{v}. \quad (2)$$

Above, E_s/N_T represents the energy transmitted per symbol (i.e., per antenna), so that E_s is the energy transmitted per channel use. The additive noise vector \mathbf{v} is zero-mean, uncorrelated, circularly-symmetric, complex Gaussian with $\mathbf{v} \sim \mathcal{CN}(\mathbf{0}, N_0 \mathbf{I}_{N_R})$. We will also employ its normalized version $\mathbf{v}_n = \mathbf{v}/\sqrt{N_0} \sim \mathcal{CN}(\mathbf{0}, \mathbf{I}_{N_R})$. We shall employ the per-symbol input SNR, defined as

$$\Gamma_s = \frac{E_s}{N_0} \frac{1}{N_T}, \quad (3)$$

as well as the per-bit input SNR, which, for a modulation constellation with M symbols (e.g., *MPSK*), is defined as

$$\Gamma_b = \frac{\Gamma_s}{\log_2 M}. \quad (4)$$

Then, $\mathbf{H} = (\mathbf{h}_1 \mathbf{h}_2 \dots \mathbf{h}_{N_T})$ is the $N_R \times N_T$ complex-Gaussian channel matrix, assumed to have rank N_T . Vector \mathbf{h}_k comprises the channel factors between transmit-antenna k and all receive-antennas. The deterministic (i.e., mean) and random components of \mathbf{H} are denoted as $\mathbf{H}_d = (\mathbf{h}_{d,1} \mathbf{h}_{d,2} \dots \mathbf{h}_{d,N_T})$ and $\mathbf{H}_r = (\mathbf{h}_{r,1} \mathbf{h}_{r,2} \dots \mathbf{h}_{r,N_T})$, respectively, so that $\mathbf{H} = \mathbf{H}_d + \mathbf{H}_r$. If $[\mathbf{H}_d]_{i,j} = 0$ then $|[\mathbf{H}]_{i,j}|$ has a Rayleigh distribution; otherwise, $|[\mathbf{H}]_{i,j}|$ has a Rician distribution [18]. Typically, the channel matrix for Rician fading is written as

$$\mathbf{H} = \mathbf{H}_d + \mathbf{H}_r = \sqrt{\frac{K}{K+1}} \mathbf{H}_{d,n} + \sqrt{\frac{1}{K+1}} \mathbf{H}_{r,n}, \quad (5)$$

where it is assumed for normalization purposes [19] that $\|\mathbf{H}_{d,n}\|^2 = N_T N_R$ and $\mathbb{E}\{|[\mathbf{H}_{r,n}]_{i,j}|^2\} = 1, \forall i, j$, so that $\mathbb{E}\{\|\mathbf{H}\|^2\} = N_T N_R$. Power ratio

$$K = \frac{\|\mathbf{H}_d\|^2}{\mathbb{E}\{\|\mathbf{H}_r\|^2\}} = \frac{\frac{K}{K+1} \|\mathbf{H}_{d,n}\|^2}{\frac{1}{K+1} \mathbb{E}\{\|\mathbf{H}_{r,n}\|^2\}} \quad (6)$$

is the Rician K -factor: $K = 0$ yields Rayleigh fading for all elements of \mathbf{H} ; $K \neq 0$ yields Rician fading if $\mathbf{H}_{d,n} \neq \mathbf{0}$.

As in [6], we view the channel matrix as partitioned into the column that affects the intended stream, i.e., Stream 1, and the matrix whose columns each affect the interfering streams, i.e.,

$$\mathbf{H} = (\mathbf{h}_1 \mathbf{H}_2) = (\mathbf{h}_{d,1} \mathbf{H}_{d,2}) + (\mathbf{h}_{r,1} \mathbf{H}_{r,2}) \quad (7)$$

and assume that $\mathbf{H}_{d,2} = \mathbf{0}$, whereas $\mathbf{h}_{d,1}$ can be nonzero, i.e., Rician-Rayleigh fading.

As a result of the above normalization and assumptions we can write

$$\|\mathbf{h}_{d,1}\|^2 = \|(\mathbf{h}_{d,1} \mathbf{0}_{N_R \times (N_T-1)})\|^2 = \|\mathbf{H}_d\|^2 = \frac{K}{K+1} N_R N_T. \quad (8)$$

We also assume zero receive-correlation but allow for nonzero transmit-correlation. Then, we assume, for tractability, as in previous work [20] [21], that all conjugate-transposed rows of $\mathbf{H}_{r,n}$ have distribution $\mathcal{CN}(\mathbf{0}, \mathbf{R}_T)$, with $[\mathbf{R}_T]_{i,i} = 1, \forall i = 1 : N_T$. Thus, all conjugate-transposed rows of \mathbf{H}_r have distribution $\mathcal{CN}(\mathbf{0}, \mathbf{R}_{T,K} = \frac{1}{K+1} \mathbf{R}_T)$. The elements of \mathbf{R}_T can be computed from the azimuth spread (AS) as shown in [22, Section VI.A] for WINNER II, i.e., Laplacian, power azimuth spectrum. Note that WINNER II has modeled both K (in dB) and AS (in degrees) as random variables with scenario-dependent lognormal distributions [4].

III. INFINITE-SERIES EXPRESSIONS FOR MIMO ZF M.G.F. AND P.D.F. [6]

A. MIMO ZF and Its SNR

For the received signal vector from (2), ZF means mapping the following vector into the closest modulation constellation symbols [1, Eq. (22)]:

$$\sqrt{\frac{N_T}{E_s}} [\mathbf{H}^H \mathbf{H}]^{-1} \mathbf{H}^H \mathbf{r} = \mathbf{x} + \frac{1}{\sqrt{\Gamma_s}} [\mathbf{H}^H \mathbf{H}]^{-1} \mathbf{H}^H \mathbf{v}_n. \quad (9)$$

Then, the ZF SNR for Stream 1 is given by

$$\gamma_1 = \frac{\Gamma_s}{[(\mathbf{H}^H \mathbf{H})^{-1}]_{1,1}}. \quad (10)$$

B. Infinite-Series Expressions for ZF SNR M.G.F. and P.D.F. [6]

The m.g.f. of γ_1 is defined as [18, Eq. (1.2)]

$$M_{\gamma_1}(s, a) = \mathbb{E}\{e^{s\gamma_1}\} = \int_0^\infty e^{st} p_{\gamma_1}(t, a) dt, \quad (11)$$

where $p_{\gamma_1}(t, a)$ is the p.d.f. of γ_1 . Thus, the m.g.f. is related to the Laplace transform [10, Eq. (1.14.17)] $L_{\gamma_1}(s, a)$ of the p.d.f. simply by a sign change, i.e.,

$$M_{\gamma_1}(-s, a) = L_{\gamma_1}(s, a) = \int_0^\infty e^{-st} p_{\gamma_1}(t, a) dt. \quad (12)$$

For MIMO ZF under Rician-Rayleigh fading we have recently obtained the following exact expression for the m.g.f. of the SNR of the Rician-fading Stream 1 [6, Eq. (31)]:

$$M_{\gamma_1}(s, a) = \frac{1}{(1 - \Gamma_1 s)^N} {}_1F_1\left(N; N_R; a \frac{\Gamma_1 s}{1 - \Gamma_1 s}\right), \quad (13)$$

where ${}_1F_1(N; N_R; \sigma)$ is the confluent hypergeometric function of scalar argument σ [10, Ch. 13], and

$$\Gamma_1 = \frac{\Gamma_s}{[\mathbf{R}_{T,K}^{-1}]_{1,1}} \propto \frac{\Gamma_s}{K+1}, \quad (14)$$

$$a = [\mathbf{R}_{T,K}^{-1}]_{1,1} \|\mathbf{h}_{d,1}\|^2 \propto K N_R N_T. \quad (15)$$

The confluent hypergeometric function has the infinite-series expression [10, Eq. (13.2.2), p. 322]

$${}_1F_1(N; N_R; \sigma) = \sum_{n=0}^{\infty} \frac{(N)_n}{(N_R)_n} \frac{\sigma^n}{n!} = \sum_{n=0}^{\infty} A_n(\sigma), \quad (16)$$

where $(N)_n$ is the Pochhammer symbol, i.e., $(N)_0 = 1$ and $(N)_n = N(N+1)\dots(N+n-1)$, $\forall n > 1$ [10, p. xiv]. A proof of the fact (important herein) that expression (16) is the expansion of ${}_1F_1(N; N_R; \sigma)$ around $\sigma = 0$ is provided, for completeness, in Appendix I.

Using (16), we have shown that (13) can be written as the infinite series [6, Eq. (37)]

$$M_{\gamma_1}(s, a) = \sum_{n=0}^{\infty} A_n(a) \sum_{m=0}^n \binom{n}{m} (-1)^m \frac{1}{(1 - s\Gamma_1)^{N+n-m}}. \quad (17)$$

Then, the SNR p.d.f. is given by the following infinite series [6, Eq. (39)]

$$p_{\gamma_1}(t, a) = \sum_{n=0}^{\infty} A_n(a) \sum_{m=0}^n \binom{n}{m} (-1)^m \frac{t^{N+n-m-1} e^{-t/\Gamma_1}}{[(N+n-m)-1]! \Gamma_1^{N+n-m}}, \quad t \geq 0. \quad (18)$$

For the special case with $N = 1$, i.e., for $N_R = N_T$, the above becomes

$$p_{\gamma_1}(t, a) = \frac{e^{-t/\Gamma_1}}{\Gamma_1} \sum_{n=0}^{\infty} A_n(a) \sum_{m=0}^n \binom{n}{m} (-1)^m \frac{t^{n-m}}{(n-m)! \Gamma_1^{n-m}}, \quad t \geq 0, \quad (19)$$

which yields

$$\lim_{t \rightarrow 0, t > 0} p_{\gamma_1}(t, a) = p_{\gamma_1}(0+, a) = \frac{1}{\Gamma_1} \sum_{n=0}^{\infty} A_n(a) (-1)^n = \frac{1}{\Gamma_1} \sum_{n=0}^{\infty} \frac{(N)_n}{(N_R)_n} \frac{(-a)^n}{n!}. \quad (20)$$

Thus, (20), (16), and (18) yield:

$$p_{\gamma_1}(0+, a) = \begin{cases} \frac{1}{\Gamma_1} {}_1F_1(N; N_R; -a), & N = 1 \\ 0, & N > 1. \end{cases} \quad (21)$$

For the special case of Rayleigh-only fading, $K = 0$ yields $a = 0$ from (15), and then only the term for $n = m = 0$ remains in (17) and (18), i.e.,

$$M_{\gamma_1}(s, 0) = \frac{1}{(1 - s\Gamma_1)^N}, \quad (22)$$

$$p_{\gamma_1}(t, 0) = \frac{t^{N-1} e^{-t/\Gamma_1}}{(N-1)! \Gamma_1^N}, \quad t \geq 0, \quad (23)$$

so that the ZF SNR is gamma-distributed.

On the other hand, for $K \neq 0$, i.e., for Rician-Rayleigh fading, (17) and (18) reveal that the ZF SNR is an infinite linear combination of gamma distributions. These m.g.f. and p.d.f. expressions have yielded infinite-series expressions in [6, Eqs. (68),(71)], respectively, for the outage probability and ergodic capacity, which are defined as follows:

$$P_o(\gamma_{1,\text{th}}, a) = Pr(\gamma_1 \leq \gamma_{1,\text{th}}) = \int_0^{\gamma_{1,\text{th}}} p_{\gamma_1}(t, a) dt, \quad (24)$$

$$C(a) = \mathbb{E}_{\gamma_1}\{C(\gamma_1)\} = \int_0^{\infty} \log_2(1+t) p_{\gamma_1}(t, a) dt. \quad (25)$$

In (24), $\gamma_{1,\text{th}}$ is the threshold-SNR.

IV. CONVENTIONAL COMPUTATION OF ${}_1F_1(\cdot; \cdot; \sigma)$ AND ENSUING LIMITATIONS

A. Recursive Computation of Truncated Infinite Series of ${}_1F_1(\cdot; \cdot; \sigma)$

Recall that the ZF SNR expression (13) depends on the confluent hypergeometric function ${}_1F_1(\cdot; \cdot; \sigma)$. Conventionally, this function has been expressed as the infinite series given in (16), which is the result of expansion around $\sigma = 0$, as detailed in Appendix I. Then, the truncation of this series has conventionally been employed to compute (i.e., accurately approximate) ${}_1F_1(\cdot; \cdot; \sigma)$.

However, computing and adding one-by-one each term $A_n(\sigma)$ of (16) is not efficient. It also encounters numerical instability even for relatively-low values of σ [11]. This is because, with increasing σ , terms for higher n have to be considered for numerical convergence. However, Pochhammer products (similarly to factorials) of large numbers are represented with large absolute error. We detailed these numerical issues in [9].

Accurate results for larger σ can be computed more efficiently through recursive methods, e.g., [11, Method 1]:

- Starting from $A_0(\sigma) = 1$, recursively update $A_n(\sigma)$ with:

$$A_n(\sigma) = A_{n-1}(\sigma) \frac{N+n-1}{N_R+n-1} \frac{\sigma}{n}, \quad n = 1, 2, 3, \dots \quad (26)$$

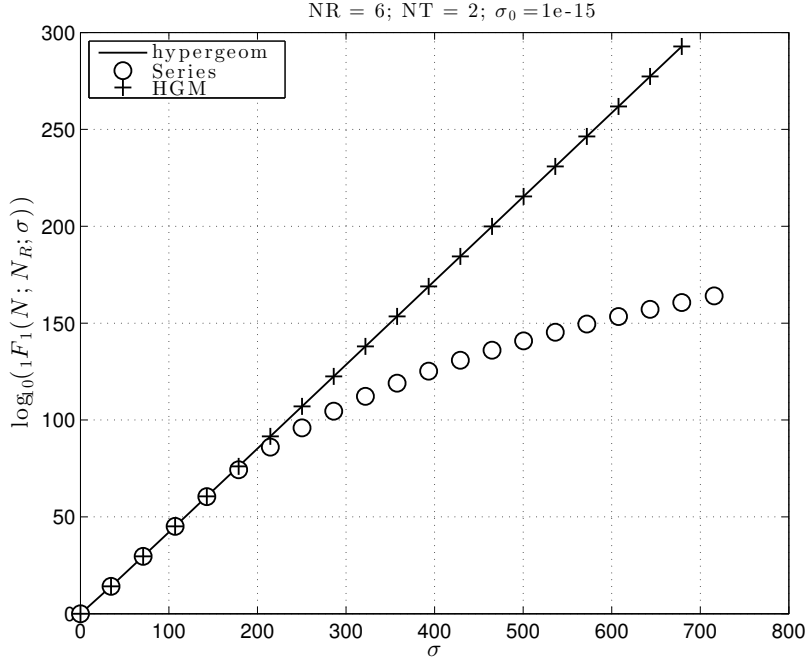


Fig. 1. $\log_{10}({}_1F_1(N; N_R; \sigma))$, for $N_R = 6$, $N_T = 2$, computed with the MATLAB `hypergeom` function, with the series (16) using the recursion (26), as well as with the system of differential equations (29) using HGM, for $\sigma_0 = 10^{-15}$.

- Stop at sufficiently large $n = n_{\max}$ (to avoid excessive computation time or numerical instability caused by the inaccuracy in representing large numbers) or when

$$\left| \frac{A_n(\sigma)}{\sum_{i=1}^n A_i(\sigma)} \right| \leq \xi, \quad (27)$$

where ξ is the tolerance level. Then, ${}_1F_1(N; N_R; \sigma) \approx \sum_{i=0}^n A_i(\sigma)$.

Nevertheless, such recursive methods converge slowly and also incur numerical instability for sufficiently-large σ [11].

We have implemented in MATLAB the recursive series-approximation method described above, for $n_{\max} = 150$ and $\xi = 10^{-15}$. We have also employed the MATLAB function `hypergeom`, whose implementation details are inaccessible. Fig. 1 depicts the obtained results, along with HGM results described later. First, these results reveal that all methods break down for sufficiently-large argument (i.e., $\sigma \approx 700$). Then, the results obtained by series truncation diverge significantly from the true value for $\sigma > 200$ because the series is an expansion around $\sigma = 0$.

B. Closed-Form and Infinite-Series Expressions for ${}_1F_1(N; N_R; \sigma)$

On the one hand, ${}_1F_1(\alpha; \beta; \sigma)$ can be represented, when $\alpha \leq \beta$ are positive integers, as a combination of two finite series [6, Eq. (35)]. Unfortunately, this closed-form expression for ${}_1F_1(N; N_R; \sigma)$ yields for the MIMO ZF SNR m.g.f. a closed-form expression [6, Eq. (36)] that cannot be Laplace-inverted to express the p.d.f. in terms of finite series. On the other hand, the infinite-series expression for ${}_1F_1(N; N_R; \sigma)$ from (16) has yielded the infinite-series expression for the MIMO ZF SNR m.g.f. from (17), which, in turn, has readily yielded the infinite-series p.d.f. expression in (18). Unfortunately, the difficulties described above for the computation of ${}_1F_1(N; N_R; \sigma)$ by truncating its infinite series (16) also affect the computation of the infinite-series p.d.f. expression in (18), as demonstrated next.

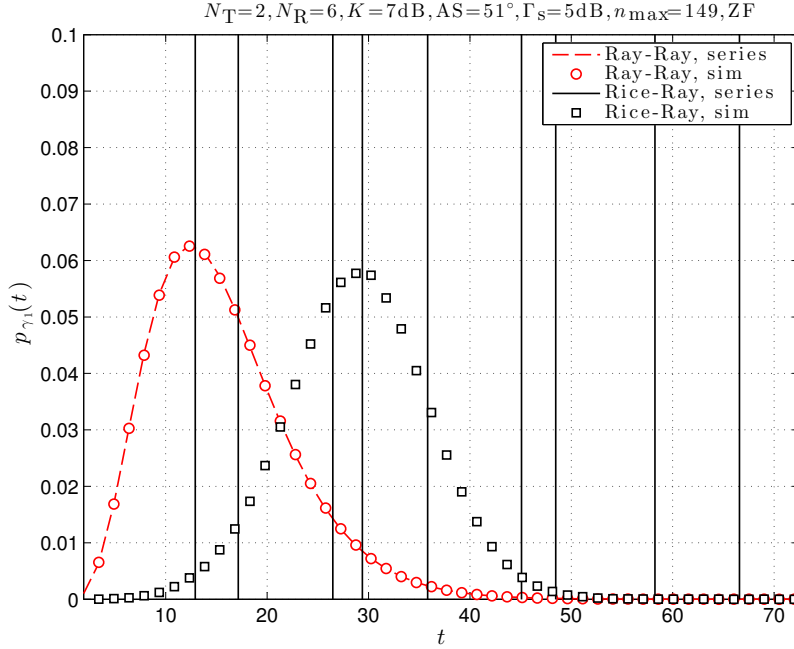


Fig. 2. P.d.f. of the SNR (in linear units) for Stream 1, for $N_R = 6$, $N_T = 2$, $K = 7$ dB, $AS = 51^\circ$, $\Gamma_s = 5$ dB.

C. Difficulties Computing the SNR P.D.F. from Infinite-Series Expression [6] [9]

As we have discussed in [6] [9], the infinite-series expression (18) cannot be computed accurately, or even at all, for large values of a (i.e., K), by truncation. This is also illustrated here in Fig. 2, for $N_R = 6$, $N_T = 2$, and $AS = 51^\circ$, which is the average AS for WINNER II scenario A1, i.e., indoor office/residential [22, Table I] [4].

For Rayleigh-only fading, i.e., for $K = 0$, results (identified in legend with `Ray-Ray`) from the infinite-series (18) — which reduces to (23) — and from simulation agree. On the other hand, for Rician-Rayleigh fading with $K = 7$ dB (identified in legend with `Rice-Ray`), the series (18) results not only do not match the simulations, but they break down at most values of t , as revealed by the vertical lines in the figures. (They connect the extreme computed values.)

Note that the value of K set for this experiment is not arbitrary: it is the average of the lognormal distribution of measured K for WINNER II indoor (office, residential) scenario A1 [22, Table I] [4]. Thus, accurately computing $p_{\gamma_1}(t)$ for $K = 7$ dB has practical relevance. However, for $N_R = 6$, $N_T = 2$, we have been able to accurately compute $p_{\gamma_1}(t)$, and, thus, the outage probability and ergodic capacity, only up to $K \approx 1.2$ dB, as detailed in [6, Sec. VI.C] [9, Sec. V]. Since series truncation cannot help compute ZF performance measures for relevant parameter values, an HGM-based approach is pursued next.

V. HOLONOMIC FUNCTIONS AND THE HOLONOMIC GRADIENT METHOD (HGM)

A. Differential Equation and HGM-Based Computation of ${}_1F_1(N; N_R; \sigma)$

It is known that ${}_1F_1(N; N_R; \sigma)$ satisfies the second-order ordinary differential¹ equation with polynomial coefficients [10, Eq. (13.2.1), p. 322]

$$\sigma \cdot {}_1F_1^{(2)}(N; N_R; \sigma) + (N_R - \sigma) \cdot {}_1F_1^{(1)}(N; N_R; \sigma) - N \cdot {}_1F_1(N; N_R; \sigma) = 0. \quad (28)$$

Because (28) can be recast as

$$\partial_\sigma \begin{pmatrix} {}_1F_1(N; N_R; \sigma) \\ {}_1F_1^{(1)}(N; N_R; \sigma) \end{pmatrix} = \begin{pmatrix} 0 & 1 \\ \frac{N}{\sigma} & 1 - \frac{N_R}{\sigma} \end{pmatrix} \begin{pmatrix} {}_1F_1(N; N_R; \sigma) \\ {}_1F_1^{(1)}(N; N_R; \sigma) \end{pmatrix}, \quad (29)$$

¹Herein, ${}_1F_1^{(k)}(N; N_R; \sigma)$ stands for the k th derivative w.r.t. σ of ${}_1F_1(N; N_R; \sigma)$.

given initial conditions, i.e., ${}_1F_1(N; N_R; \sigma_0)$ and ${}_1F_1^{(1)}(N; N_R; \sigma_0)$ for some σ_0 , one can compute ${}_1F_1(N; N_R; \sigma)$ for any σ by solving (29) numerically² between σ_0 and σ .

Unfortunately, because σ multiplies ${}_1F_1^{(2)}(N; N_R; \sigma)$ in (28), i.e., it appears in denominators in (29), one cannot use the initial value $\sigma_0 = 0$ and the initial conditions ${}_1F_1(N; N_R; 0) = 1$ and ${}_1F_1^{(1)}(N; N_R; 0) = \frac{N}{N_R}$ ensuing from (16). Therefore, the initial conditions ${}_1F_1(N; N_R; \sigma_0)$ and ${}_1F_1^{(1)}(N; N_R; \sigma_0) = \frac{N}{N_R} {}_1F_1(N + 1; N_R + 1; \sigma_0)$ [10, Eq. (13.3.15), p. 325] have to be obtained numerically for some $\sigma_0 > 0$ by series (16) truncation, as discussed in Section IV-A. Nevertheless, since σ_0 can be selected arbitrarily small, we can achieve high accuracy.

Thus, HGM for the computation of ${}_1F_1(N; N_R; \sigma)$ proceeds as follows:

- First, compute accurate initial conditions, i.e., ${}_1F_1(N; N_R; \sigma_0)$ and ${}_1F_1^{(1)}(N; N_R; \sigma_0)$, for some sufficiently-small $\sigma_0 > 0$, by infinite-series truncation.
- Then, solve numerically the system of differential equations (29) between σ_0 and σ .

For example, the above approach starting at $\sigma_0 = 10^{-15}$ has yielded the results identified with HGM in Fig. 1. They agree with the results from the MATLAB `hypergeom` function (but the latter required orders-of-magnitude larger computation time for large σ).

B. Holonomic Functions: Definition and Properties

Definition 1 ([16, Section 2]): A function that satisfies, w.r.t. each variable, an ordinary differential equation with polynomial coefficients is referred to as *holonomic*.

Simple examples of holonomic functions are the polynomial and exponential-polynomial functions [12, Section 2.5]. The confluent hypergeometric function ${}_1F_1(N; N_R; \sigma)$ is holonomic because it satisfies (28).

Proposition 1 ([12, Proposition 2.1]): If $f(x)$ is a polynomial then $1/f(x)$ is holonomic.

Proposition 2 ([13, Theorem 1.4.2, p. 16]): If $f(x)$ is holonomic and $h(x)$ is a rational function then $f(h(x))$ is holonomic.

Proposition 3 ([12, Proposition 3.2]): If $f(x)$ and $g(x)$ are holonomic then their multiplication $f(x)g(x)$ is also holonomic.

Proposition 4 ([12, p. 337]): If $f(x)$ is holonomic then its Fourier transform is holonomic.

Based on the above properties, in the SNR m.g.f. expression (13), the first term

$$\frac{1}{(1 - \Gamma_1 s)^N}$$

is holonomic w.r.t. s , and the second term

$${}_1F_1\left(N; N_R; a \frac{\Gamma_1 s}{1 - \Gamma_1 s}\right) \quad (30)$$

is holonomic w.r.t. both s and a . These yield the following property.

Lemma 1: The SNR m.g.f. $M_{\gamma_1}(s, a)$ described by expression (13) is holonomic w.r.t. both s and a , i.e., it must satisfy ordinary differential equations with polynomial coefficients w.r.t. both s and a . Also, the ZF SNR p.d.f. $p_{\gamma_1}(t, a)$ is holonomic w.r.t. both t and a , i.e., it must satisfy ordinary differential equations with polynomial coefficients w.r.t. both t and a .

Therefore, the remainder of this work is devoted to:

- Obtaining the differential equations (known to exist) satisfied by $M_{\gamma_1}(s, a)$, w.r.t. both s and a , as well as by $p_{\gamma_1}(t, a)$, w.r.t. both t and a .
- Exploiting the differential equations for the SNR p.d.f. $p_{\gamma_1}(t, a)$ in HGM to accurately compute ZF performance measures for practically-relevant values of K .

²E.g., with the `ode` function, in MATLAB.

VI. DIFFERENTIAL EQUATIONS FOR ZF SNR M.G.F. AND P.D.F.

A. M.G.F. and P.D.F. Variable Scaling

In order to simplify notation and derivations hereafter, let us denote the m.g.f. $M_{\gamma_1}(s, a)$ and the p.d.f. $p_{\gamma_1}(t, a)$ for $\Gamma_1 = 1$ as $M(s, a)$ and $p(t, a)$, respectively. Now, by definition, we have

$$M_{\gamma_1}(s, a) = \mathbb{E}\{e^{s\gamma_1}\} = \int_0^\infty e^{st} p_{\gamma_1}(t, a) dt, \quad (31)$$

$$M(s, a) = \int_0^\infty e^{st} p(t, a) dt. \quad (32)$$

Then, because

$$M_{\gamma_1}(s, a) = M(s\Gamma_1, a) = \int_0^\infty e^{s\Gamma_1 t} p(t, a) dt = \int_0^\infty e^{sy} \frac{1}{\Gamma_1} p(y/\Gamma_1, a) dy,$$

the p.d.f. $p_{\gamma_1}(t, a)$ of γ_1 for any Γ_1 can be obtained from $p(t, a)$ as follows:

$$p_{\gamma_1}(t, a) = \frac{1}{\Gamma_1} p(t/\Gamma_1, a). \quad (33)$$

Thus, below, we first derive differential equations for $M(s, a)$ w.r.t. both s and a . From them we then deduce differential equations for $p(t, a)$ w.r.t. both t and a . They will help compute, by HGM, the function $p(t, a)$ at desired values of t and a (i.e., K). Finally, the scaling transformation from (33) will return the value of the SNR p.d.f. $p_{\gamma_1}(t, a)$, for any Γ_1 .

B. Differential Equation w.r.t. s for $M(s, a)$

Based on (13) and (31) we can write

$$M(s, a) = \frac{1}{(1-s)^N} {}_1F_1 \left(N; N_{\mathbf{R}}; \frac{as}{1-s} \right). \quad (34)$$

In Appendix II, manipulation and differentiation w.r.t. s of (34) followed by substitution into the differential equation for ${}_1F_1(N; N_{\mathbf{R}}; \sigma)$ from (28) yield the following differential equation w.r.t. s for $M(s, a)$, in (94):

$$(s(1-s)^2 \partial_s^2 - [2(N+1)s(1-s) - (1-s)N_{\mathbf{R}} + as] \partial_s + N[(N+1)s - N_{\mathbf{R}} - a]) M(s, a) = 0. \quad (35)$$

Because s^l appears in front of ∂_s^k in (35), the corresponding differential equation for $p(t, a)$ cannot be obtained directly. Therefore, we shall employ the following order-changing rule, which can readily be deduced from [15, Th. 6.1.2 (Liebniz Formula), p. 282] [23, Th. 1.1.1, p. 3].

Proposition 5:

$$s^l \partial_s^k = \sum_{m=0}^{\min(l,k)} (-1)^m \frac{l(l-1)\dots(l-m+1)k(k-1)\dots(k-m+1)}{m!} \partial_s^{k-m} s^{l-m}. \quad (36)$$

From (36) we obtain the following particular rules

$$s \partial_s = \partial_s s - 1, \quad (37)$$

$$s \partial_s^2 = \partial_s^2 s - 2 \partial_s, \quad (38)$$

$$s^2 \partial_s = \partial_s s^2 - 2s, \quad (39)$$

$$s^2 \partial_s^2 = \partial_s^2 s^2 - 4 \partial_s s + 2, \quad (40)$$

$$s^3 \partial_s^2 = \partial_s^2 s^3 - 6 \partial_s s^2 + 6s, \quad (41)$$

which, when applied in (35) yield for $M(s, a)$ the following differential equation w.r.t. s :

$$\begin{aligned} & [\partial_s^3 s^3 - 2 \partial_s^2 s^2 + \partial_s^2 s + (2N-4) \partial_s s^2 + (6-2N-N_{\mathbf{R}}-a) \partial_s s + (N_{\mathbf{R}}-2) \partial_s \\ & + (N-1)(N-2)s + (N-1)(2-N_{\mathbf{R}}-a)] M(s, a) = 0. \end{aligned} \quad (42)$$

C. Differential Equation w.r.t. t for $p(t, a)$

The following proposition helps transform an expression whereby the operator ∂_s^k is applied to the product $s^l M(s, a)$ into a differential equation³ for $p(t, a)$ w.r.t. t .

Proposition 6: The integral $\int_0^\infty e^{st} [t^k p^{(l)}(t, a)] dt$, which represents the Laplace transform of $t^k p^{(l)}(t, a)$ for argument $-s$, is given by:

$$\begin{cases} (-1)^l \partial_s^k [s^l M(s, a)] + \sum_{m=k+1}^l (-1)^m p^{(l-m)}(0+, a) \frac{(m-1)!}{(m-k-1)!} s^{m-k-1}, & l \geq 1, \\ \partial_s^k M(s, a), & l = 0. \end{cases} \quad (43)$$

Proof: Follows from the well-known Laplace-transform property for higher-order derivatives from [10, Eq. (1.14.29), p. 28] and the sign change from (12).

Using (43) appropriately for the terms in (42) yields the following Laplace transform pairs:

$$\begin{aligned} \partial_s^2 s^3 M(s, a) + 2! p(0+, a) &\leftrightarrow -t^2 p^{(3)}(t, a) \\ -2\partial_s^2 s^2 M(s, a) &\leftrightarrow -2t^2 p^{(2)}(t, a) \\ \partial_s^2 s M(s, a) &\leftrightarrow -t^2 p^{(1)}(t, a) \\ (2N - 4)\partial_s s^2 M(s, a) + (2N - 4) p(0+, a) &\leftrightarrow (2N - 4) t p^{(2)}(t, a) \\ (6 - 2N - N_R - a) \partial_s s M(s, a) &\leftrightarrow -(6 - 2N - N_R - a) t p^{(1)}(t, a) \\ (N_R - 2)\partial_s M(s, a) &\leftrightarrow (N_R - 2) t p(t, a) \\ (N - 1)(N - 2)s M(s, a) + (N - 1)(N - 2)p(0+, a) &\leftrightarrow -(N - 1)(N - 2) p^{(1)}(t, a) \\ (N - 1)(2 - N_R - a) M(s, a) &\leftrightarrow (N - 1)(2 - N_R - a) p(t, a). \end{aligned}$$

Summing the left-hand side terms (i.e., the s -domain terms) of the above transform pairs and accounting for (42) yields the constant $N(N - 1)p(0+, a)$, which reduces to 0 for any $N \geq 1$ because, based on (21) and (33), we have:

$$p(0+, a) = \begin{cases} {}_1F_1(N; N_R; -a), & N = 1, \\ 0, & N > 1. \end{cases} \quad (44)$$

Then, by the uniqueness of the Laplace transform, the right-hand side terms (i.e., the t -domain terms) of the above transform pairs also sum to 0, i.e.,

$$\begin{aligned} -t^2 p^{(3)}(t, a) - 2t^2 p^{(2)}(t, a) - t^2 p^{(1)}(t, a) + (2N - 4) t p^{(2)}(t, a) - (6 - 2N - N_R - a) t p^{(1)}(t, a) \\ + (N_R - 2) t p(t, a) - (N - 1)(N - 2) p^{(1)}(t, a) + (N - 1)(2 - N_R - a) p(t, a) = 0. \end{aligned} \quad (45)$$

This differential equation w.r.t. t for $p(t, a)$ can be rewritten more compactly as

$$\begin{aligned} p^{(3)}(t, a) &= \frac{(N_R - 2)t + (N - 1)(2 - N_R - a)}{t^2} p(t, a) \\ &\quad - \frac{t^2 + (6 - 2N - N_R - a)t + (N - 1)(N - 2)}{t^2} p^{(1)}(t, a) \\ &\quad - \frac{2t^2 - (2N - 4)t}{t^2} p^{(2)}(t, a). \end{aligned} \quad (46)$$

³Herein, $p^{(l)}(t, a)$ stands for the l th derivative w.r.t. t of $p(t, a)$.

D. Computation of $p(t, a)$ vs. t , Given a , by HGM w.r.t. t

By defining the function vector

$$\mathbf{p}(t, a) = (p(t, a) \quad p^{(1)}(t, a) \quad p^{(2)}(t, a))^T, \quad (47)$$

we can recast (46) as the system of differential equations w.r.t. t

$$\partial_t \mathbf{p}(t, a) = \mathbf{P}(t, a) \mathbf{p}(t, a), \quad (48)$$

where the elements of the 3×3 companion matrix $\mathbf{P}(t, a)$ are as follows:

$$[\mathbf{P}(t, a)]_{1,1} = [\mathbf{P}(t, a)]_{1,3} = 0 \quad (49)$$

$$[\mathbf{P}(t, a)]_{2,1} = [\mathbf{P}(t, a)]_{2,2} = 0 \quad (50)$$

$$[\mathbf{P}(t, a)]_{1,2} = [\mathbf{P}(t, a)]_{2,3} = 1 \quad (51)$$

$$[\mathbf{P}(t, a)]_{3,1} = \frac{(N_R - 2)t + (N - 1)(2 - N_R - a)}{t^2} \quad (52)$$

$$[\mathbf{P}(t, a)]_{3,2} = -\frac{t^2 + (6 - 2N - N_R - a)t + (N - 1)(N - 2)}{t^2} \quad (53)$$

$$[\mathbf{P}(t, a)]_{3,3} = -\frac{2t^2 - (2N - 4)t}{t^2}. \quad (54)$$

Now, since we are interested in computing the SNR p.d.f. over a relevant range of t , as depicted in Fig. 2, an HGM-based procedure based on (48) would suit naturally, because it inherently computes $p(t, a)$ over a range of interest for t , for a given a , as follows. Given the initial condition $\mathbf{p}(t_0, a) = (p(t_0, a) \quad p^{(1)}(t_0, a) \quad p^{(2)}(t_0, a))^T$ for a certain t_0 , the system of differential equations (48) is solved numerically between t_0 and t . Note that HGM requires $t_0 \neq 0$ because t appears in denominators of the elements of $\mathbf{P}(t, a)$. Then, the computation of $p(t_0, a)$, $p^{(1)}(t_0, a)$, and $p^{(2)}(t_0, a)$ may be attempted from their infinite-series expressions derived in Appendix III. However, this approach is reliable only for a sufficiently-small (i.e., practically-irrelevant). To compute $\mathbf{p}(t_0, a)$ at relevant values of a , an HGM-based approach needs to be pursued based on the differential equation w.r.t. a for $p(t, a)$, which is known to exist, and which is derived next.

E. Differential Equation w.r.t. a for $p(t, a)$

In Appendix IV, Eq. (108), we have deduced the relationship

$$a\partial_a M(s, a) = (s\partial_s - s^2\partial_s - Ns) M(s, a). \quad (55)$$

which, by using the order-changing rules (37) and (39), becomes

$$\begin{aligned} a\partial_a M(s, a) &= (\partial_s s - 1 - \partial_s s^2 + 2s - Ns) M(s, a) \\ &= [-1 + (-Ns + \partial_s s + 2s) - \partial_s s^2] M(s, a). \end{aligned} \quad (56)$$

Transforming (56) from the s -domain to the t -domain based on (43) yields

$$\begin{aligned} a\partial_a p(t, a) &= \underbrace{(N - 1)p(0+, a)}_{=0, \forall N} - p(t, a) + (N - t - 2)p^{(1)}(t, a) - tp^{(2)}(t, a) \\ &= -p(t, a) + (N - t - 2)p^{(1)}(t, a) - tp^{(2)}(t, a). \end{aligned} \quad (57)$$

Now, differentiating (57) w.r.t. t and then substituting $p^{(3)}(t, a)$ from (46) yields:

$$\begin{aligned}
a\partial_a p^{(1)}(t, a) &= -t p^{(3)}(t, a) + (N - t - 3) p^{(2)}(t, a) - 2p^{(1)}(t, a) \\
&= \left(2 - N_R + \frac{2 - 2N - N_R - a + NN_R + Na}{t} \right) p(t, a) \\
&\quad + \left(4 - 2N - N_R - a + t + \frac{2 + N^2 - 3N}{t} \right) p^{(1)}(t, a) \\
&\quad + (1 - N + t) p^{(2)}(t, a).
\end{aligned} \tag{58}$$

Finally, differentiating (58) w.r.t. t and then substituting $p^{(3)}(t, a)$ from (46) yields:

$$\begin{aligned}
a\partial_a p^{(2)}(t, a) &= \left(-2 + N_R + \frac{-4 + 4N + 2N_R + a - 2NN_R - Na}{t} \right. \\
&\quad \left. + \frac{-4 + 6N + 2N_R + 2a - 3NN_R - 3Na + N^2N_R + N^2a - 2N^2}{t^2} \right) p(t, a) \\
&\quad + \left(3N - 4 + a - t + \frac{-6 - 3N^2 + 9N}{t} + \frac{-4 + 8N - 5N^2 + N^3}{t^2} \right) p^{(1)}(t, a) \\
&\quad + \left(-1 + 2N - N_R - a - t + \frac{-2 - N^2 + 3N}{t} \right) p^{(2)}(t, a).
\end{aligned} \tag{59}$$

F. Computation of $p(t, a)$ vs. a , Given t , by HGM w.r.t. a

Collecting (57)–(59) yields for the function vector $\mathbf{p}(t, a)$ defined in (48) the system of differential equations w.r.t. a

$$\partial_a \mathbf{p}(t, a) = \frac{1}{a} \mathbf{Q}(t, a) \mathbf{p}(t, a), \tag{60}$$

where the elements of 3×3 matrix $\mathbf{Q}(t, a)$ are:

$$[\mathbf{Q}(t, a)]_{1,1} = -1 \tag{61}$$

$$[\mathbf{Q}(t, a)]_{1,2} = N - t - 2 \tag{62}$$

$$[\mathbf{Q}(t, a)]_{1,3} = -t \tag{63}$$

$$[\mathbf{Q}(t, a)]_{2,1} = 2 - N_R + \frac{2 - 2N - N_R - a + NN_R + Na}{t} \tag{64}$$

$$[\mathbf{Q}(t, a)]_{2,2} = 4 - 2N - N_R - a + t + \frac{2 + N^2 - 3N}{t} \tag{65}$$

$$[\mathbf{Q}(t, a)]_{2,3} = 1 - N + t \tag{66}$$

$$\begin{aligned}
[\mathbf{Q}(t, a)]_{3,1} &= -2 + N_R + \frac{-4 + 4N + 2N_R + a - 2NN_R - Na}{t} \\
&\quad + \frac{-4 + 6N + 2N_R + 2a - 3NN_R - 3Na + N^2N_R + N^2a - 2N^2}{t^2}
\end{aligned} \tag{67}$$

$$[\mathbf{Q}(t, a)]_{3,2} = 3N - 4 + a - t + \frac{-6 - 3N^2 + 9N}{t} + \frac{-4 + 8N - 5N^2 + N^3}{t^2} \tag{68}$$

$$[\mathbf{Q}(t, a)]_{3,3} = -1 + 2N - N_R - a - t + \frac{-2 - N^2 + 3N}{t}. \tag{69}$$

Now, the system of differential equations (60) may be solved numerically between some⁴ a_0 and the desired a , given t and an initial condition $\mathbf{p}(t, a_0) = (p(t, a_0) \ p^{(1)}(t, a_0) \ p^{(2)}(t, a_0))^T$ whose elements can be computed accurately for sufficiently-small a_0 from the infinite-series expressions in Appendix III.

⁴Note that a_0 cannot be 0 because a divides matrix \mathbf{Q} in (60).

This HGM-based approach w.r.t. a may be applied to compute $\mathbf{p}(t, a)$ either 1) between a_0 and a at samples of interest in the range of interest for t , or 2) between a_0 and a to compute the initial condition $\mathbf{p}(t_0, a)$, followed by the application between t_0 and t of the HGM-based approach w.r.t. t from Section VI-D. However, numerical results (unshown due to length limitations) have revealed that neither approach computes $p(t, a)$ accurately in the upper range of t . Note that these approaches proceed along axes in the (t, a) -plane. In order to improve numerical accuracy, next, we combine (48) and (60) and compute $p(t, a)$ along a line of slope $0 < c < \infty$ in the (t, a) -plane.

G. Computation of $p(t, a)$ vs. t , by HGM w.r.t. t for $a = ct$

In the systems of differential equations obtained in (48) and (60), i.e., in

$$\partial_t \mathbf{p}(t, a) = \mathbf{P}(t, a) \mathbf{p}(t, a), \quad (70)$$

$$\partial_a \mathbf{p}(t, a) = \frac{1}{a} \mathbf{Q}(t, a) \mathbf{p}(t, a), \quad (71)$$

we now make the following changes of variables

$$t = c_1 u, \quad (72)$$

$$a = c_2 u. \quad (73)$$

Then, the bivariate function vector from (47) becomes the univariate function vector

$$\mathbf{p}(c_1 u, c_2 u) = \begin{pmatrix} p(c_1 u, c_2 u) \\ p^{(1)}(c_1 u, c_2 u) \\ p^{(2)}(c_1 u, c_2 u) \end{pmatrix} = \tilde{\mathbf{p}}(u). \quad (74)$$

Based on the chain rule [10, Eq. (1.5.7), p. 7] as well as (70) and (71), we can write:

$$\begin{aligned} \frac{d}{du} \tilde{\mathbf{p}}(u) &= \frac{d}{du} \mathbf{p}(\underbrace{c_1 u}_t, \underbrace{c_2 u}_a) = \left[\partial_t \mathbf{p}(t, a) \frac{dt}{du} + \partial_a \mathbf{p}(t, a) \frac{da}{du} \right] \Bigg|_{\substack{t=c_1 u \\ a=c_2 u}} \\ &= c_1 \mathbf{P}(c_1 u, c_2 u) \tilde{\mathbf{p}}(u) + c_2 \frac{1}{c_2 u} \mathbf{Q}(c_1 u, c_2 u) \tilde{\mathbf{p}}(u) \\ &= c_1 \mathbf{P}(c_1 u, c_2 u) \tilde{\mathbf{p}}(u) + \frac{1}{u} \mathbf{Q}(c_1 u, c_2 u) \tilde{\mathbf{p}}(u). \end{aligned} \quad (75)$$

Then, for example, for $c_1 = 1$ and $c_2 = c$, we obtain the system of differential equations

$$\frac{d}{du} \tilde{\mathbf{p}}(u) = \mathbf{R}(u) \tilde{\mathbf{p}}(u), \quad (76)$$

where $\mathbf{R}(u) = \mathbf{P}(u, cu) + \frac{1}{u} \mathbf{Q}(u, cu)$ is a 3×3 matrix.

VII. NUMERICAL RESULTS

For the numerical results described below, we have used the following procedure. Given the per-symbol input SNR Γ_s , which is defined in (3), and the Rician K -factor, we computed Γ_1 and a with (14) and (15), respectively. Then, we computed the ZF SNR p.d.f. over the relevant SNR range by employing the HGM ensuing from (76) as follows:

- Compute the initial condition $\tilde{\mathbf{p}}(u_0)$ by replacing both t and a with a sufficiently-small u_0 so that $(p(u_0, u_0) \ p^{(1)}(u_0, u_0) \ p^{(2)}(u_0, u_0))^T$ is computed accurately based on the infinite series for $p^{(q)}(t, a)$ from (98)–(100) in Appendix III.
- Sample the range of interest $[u_1, u_M]$ for u , i.e., t , as: u_1, \dots, u_M .
- For each sample $u = u_m$, $m = 1 : M$:
 - 1) Set $c = a/u$.

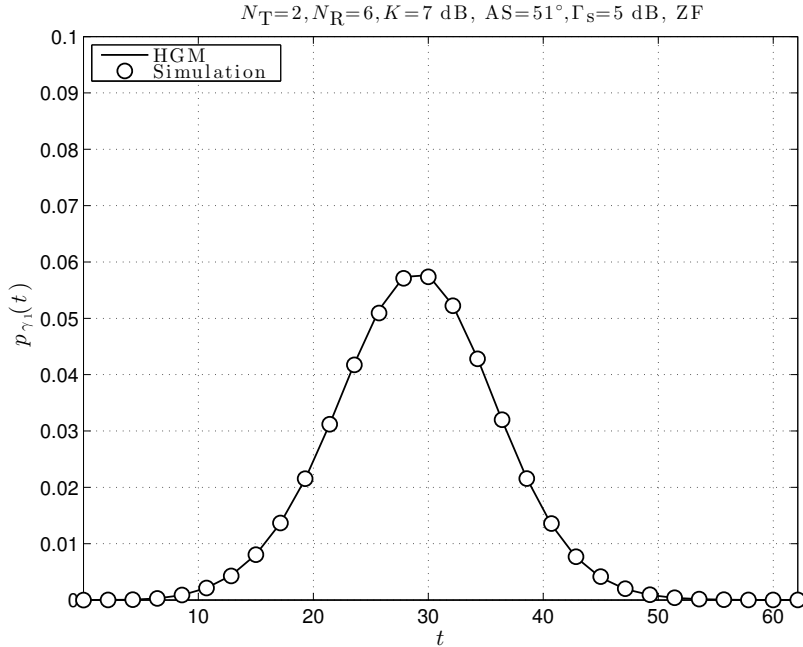


Fig. 3. Stream-1 SNR p.d.f. computed with HGM and by simulation, for $N_R = 6$, $N_T = 2$, $K = 7$ dB.

2) Solve the system of differential equations (76) from u_0 to u .

3) Save $p(u, cu)$, which represents $p(t, a)$ on the line $a = ct$.

- Finally, recover the ZF SNR p.d.f. based on (33), i.e., with $p_{\gamma_1}(t, a) = p(t/\Gamma_1, a)/\Gamma_1$.

Figs. 3 and 4 depict the SNR p.d.f. and c.d.f. computed with the HGM as above, and by simulation, for $N_R = 6$, $N_T = 2$, and $K = 7$ dB. (Since the computation of $p_{\gamma_1}(t, a)$ based on its infinite series expression (18) breaks down, we no longer try to plot its results.) HGM performs well, i.e., the resulting p.d.f. and c.d.f. plots agree with the simulation results. Also, the c.d.f. shown in Fig 4 goes to 1 for increasing t , as required.

Figs. 5 and 6 depict, respectively, the MIMO ZF outage probability and ergodic capacity. For Rayleigh-only fading, they show results from simulation as well as from expressions⁵. On the other hand, for Rician-Rayleigh fading with $K = 7$ dB, they show results from simulation and from the numerical integration of $p_{\gamma_1}(t, a)$ computed with HGM as described above, based on (24) and (25). The simulation and HGM-based results agree closely.

Results from the infinite-series expressions [6, Eqs. (69),(71)] could not be shown for $K = 7$ dB because they fall outside the displayed P_o and C ranges. In fact, our attempts to compute the infinite-series P_o and C expressions [6, Eqs. (69),(71)] with a recursive method analogous to that described for ${}_1F_1(\cdot; \cdot; \cdot)$ in Section IV-A have been successful only up to $K \approx 1.2$ dB — recall the p.d.f. results from Section IV-C and see for details [6, Sections V.F, VI.C].

VIII. OTHER RELEVANT HGM APPLICATIONS, AND FUTURE WORK

A. HGM-Based Computation of BPSK Error Probability (i.e., Q -Function)

Given the symbol-detection SNR, e.g., γ_1 , the bit error probability for BPSK modulation is given by [24, Eqn. 5.2-57, p. 268]

$$P_e(\gamma_1) = Q\left(\sqrt{2\gamma_1}\right) = \frac{1}{2} [1 - \text{erf}(\sqrt{\gamma_1})], \quad (77)$$

⁵ [6, Eqs. (69) and (71)], with $a = 0$, i.e., for $n = m = 0$.

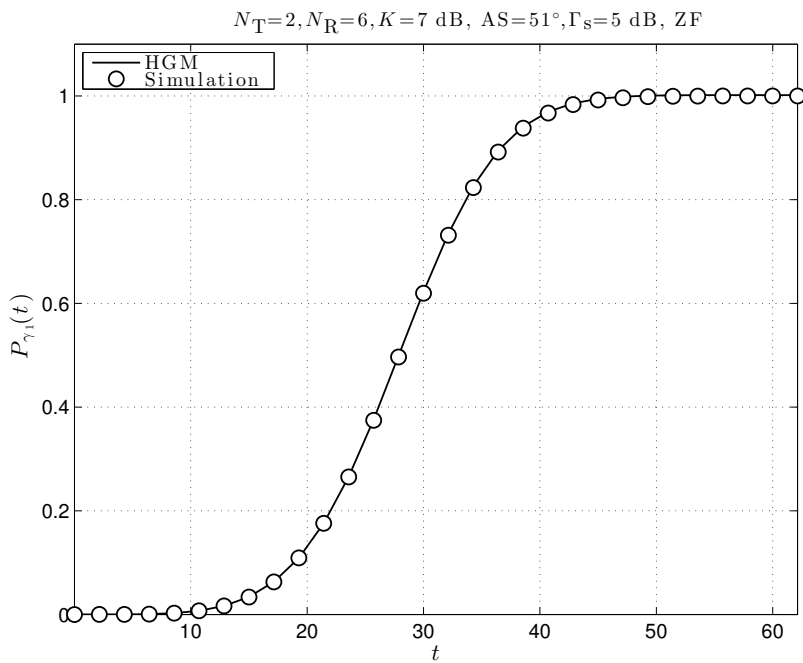


Fig. 4. Stream-1 SNR c.d.f. computed with HGM and by simulation, for $N_R = 6$, $N_T = 2$, $K = 7$ dB.

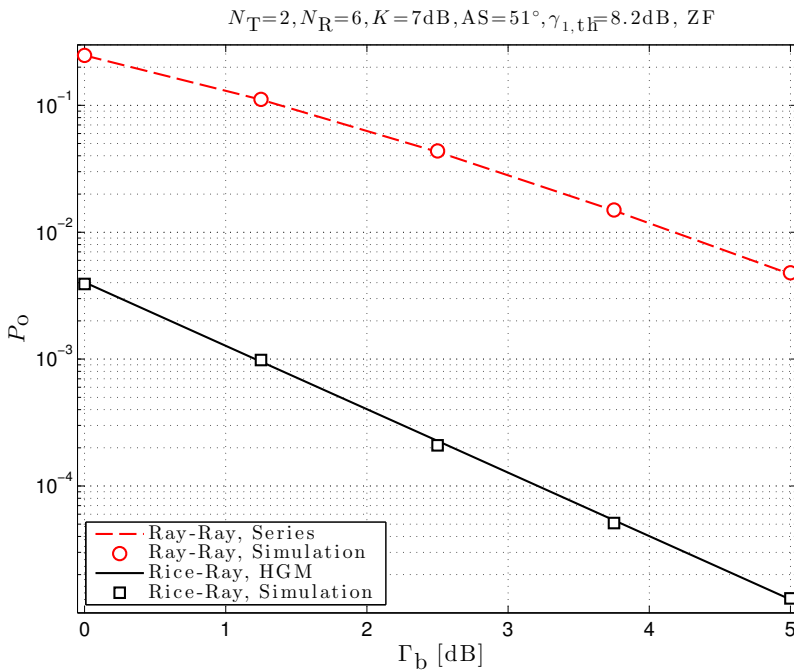


Fig. 5. Stream-1 SNR outage probability, for $N_R = 6$, $N_T = 2$, $K = 7$ dB.

where $Q(\cdot)$ is the Gaussian Q-function [18, Eqn. 4.1, p. 70], and erf is the error function⁶ [10, Eq. (7.2.1), p. 160]:

$$\text{erf}(x) = \frac{2}{\sqrt{\pi}} \int_0^x e^{-y^2} dy. \quad (78)$$

⁶Note that erf, i.e., the Q-function, can be expressed in terms of ${}_1F_1(\cdot; \cdot; \cdot)$, based on [10, Eq. (7.11.4), p. 164].

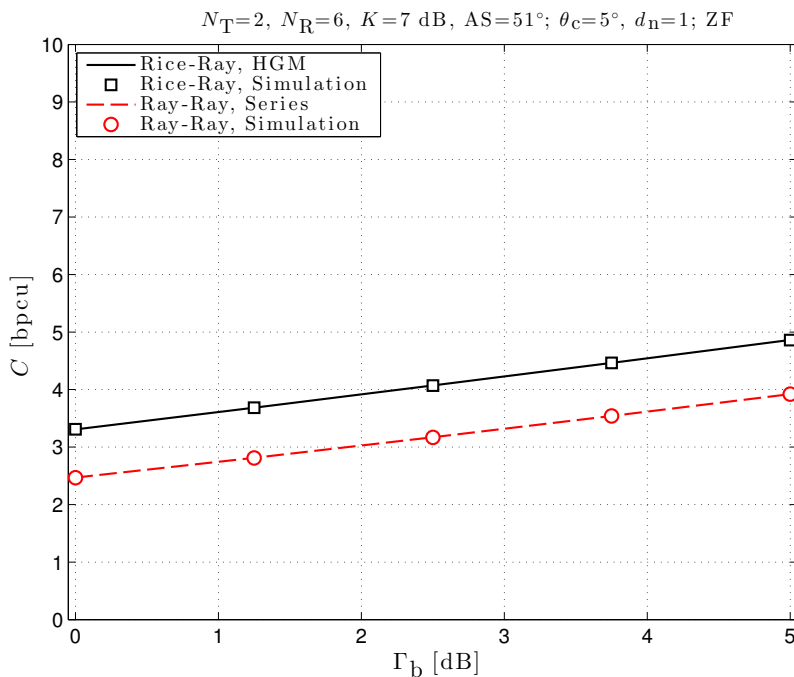


Fig. 6. Stream-1 SNR ergodic capacity, for $N_R = 6, N_T = 2, K = 7$ dB.

Now, if we write

$$E(x) = \operatorname{erf}(x) = \frac{2}{\sqrt{\pi}} \int_0^x e^{-y^2} dy = \frac{2}{\sqrt{\pi}} [F(x) - F(0)], \quad E(0) = 0, \quad (79)$$

where $F'(x) = e^{-x^2}$, then, by differentiating (79) twice, we obtain:

$$E'(x) = \frac{2}{\sqrt{\pi}} F'(x) = \frac{2}{\sqrt{\pi}} e^{-x^2}, \quad E'(0) = \frac{2}{\sqrt{\pi}}, \quad (80)$$

$$E''(x) = -2x \frac{2}{\sqrt{\pi}} e^{-x^2} = -2xE'(x). \quad (81)$$

Differential equation (81) can be solved numerically starting at $x_0 = 0$, using the initial conditions from (79) and (80), to obtain $E(x)$ at any value of x , i.e., $P_e(\gamma_1)$ from (77) at any γ_1 . The results of this approach are identified with HGM in Fig. 7. They agree closely with the ones from the native `erf` function in MATLAB, whose implementation details are inaccessible.

B. HGM-Based Computation of Hypergeometric Functions of Matrix Argument

Hypergeometric functions of matrix argument occur in analyses involving random matrix theory [25] [26]. Thus, they frequently occur in MIMO analyses due to statistical assumptions about the MIMO channel matrix. For example, the c.d.f. and m.g.f. of the dominant eigenvalue of a central-Wishart distributed matrix have been expressed in terms of ${}_1F_1(a; c; \mathbf{R})$ and ${}_2F_1(a; c; \mathbf{R})$ in [26, Eqs. (34), (42)], respectively. Thus, for binary signaling, MIMO Rayleigh fading, maximal-ratio combining, and coherent detection, the average error probability and outage probability have been expressed in terms of ${}_1F_1(a; c; \mathbf{R})$ and ${}_2F_1(a; c; \mathbf{R})$ in [26, Eqs. (30), (22)], respectively. However, the expressions typically employed for these functions involve zonal polynomials [27, Eq. (1.1)] [25, Eq. (1.1)] [26, Eq. (61)], which renders computation difficult [25] [26, p. 743].

These difficulties can be avoided by deploying HGM based on the differential equations satisfied by such functions: those for ${}_2F_1(a, b; c; \mathbf{R})$ and ${}_1F_1(a; c; \mathbf{R})$ were deduced by Muirhead in [27, Eqs. (1.3),

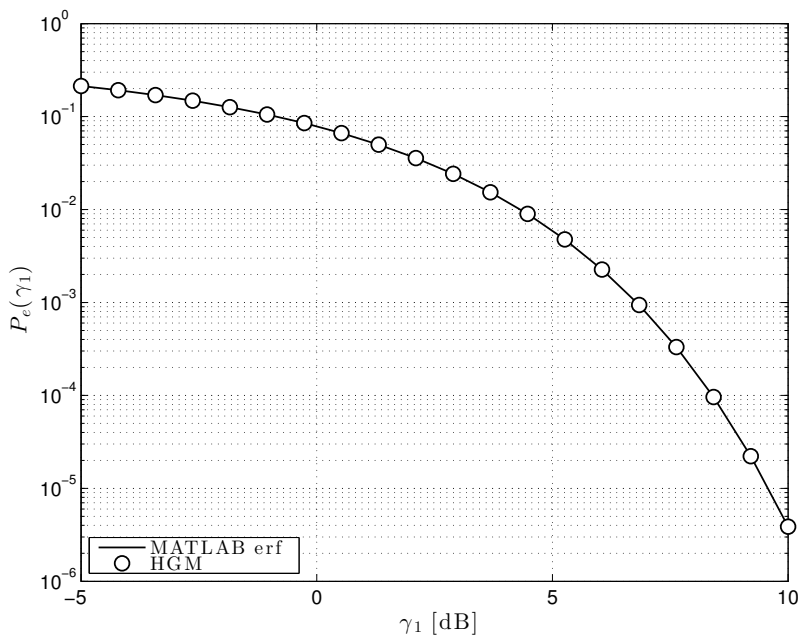


Fig. 7. BPSK error probability results obtained from (77).

(5.1)], respectively; those for other such functions relevant to MIMO analysis appear in [27, Eq. (5.2)] [28, p. 51]. Thus, the differential equations satisfied by ${}_1F_1(c; \mathbf{R})$ [27, Eq. (5.1)] have recently been employed to accurately compute by HGM the c.d.f. of the dominant eigenvalue of a (real-valued) central-Wishart-distributed matrix in [17].

C. Automated Deduction of Differential Equations for MIMO Performance Measures

We familiarized ourselves with the HGM procedure by opting herein to manually deduce the differential equations satisfied by the ZF SNR m.g.f. from the differential equation w.r.t. σ satisfied by ${}_1F_1(N; N_R; \sigma)$. Nevertheless, software tools that can automate the deduction of differential equations for holonomic functions ensuing from ${}_1F_1(N; N_R; \sigma)$, for specified values of N and N_R , have recently become available [14, p. 171] [15, Ch. 7] [29]. They shall be effectively employed in future work, also to deduce differential equations for the outage probability and ergodic capacity of MIMO ZF.

IX. SUMMARY AND CONCLUSIONS

For MIMO ZF under Rician-Rayleigh fading with realistic parameter values, this paper demonstrates that HGM helps compute accurately the performance measures. For the ZF SNR m.g.f. known in terms of the confluent hypergeometric function, we deduced the satisfied differential equations. From them, we deduced the differential equations satisfied by the SNR p.d.f. and used these equations to compute the p.d.f. with the HGM. Finally, we computed the ZF outage probability and ergodic capacity by numerically integrating the SNR p.d.f. obtained by HGM. Thus, we have been able to evaluate the MIMO ZF performance under Rician-Rayleigh fading for realistic K -factor values, which had been impossible by infinite-series truncation. Our approach may help accurately evaluate MIMO performance for heterogeneous cell deployments.

APPENDIX I

INFINITE-SERIES EXPRESSION FOR ${}_1F_1(N; N_R; \sigma)$ IS EXPANSION AROUND $\sigma = 0$

For $N_R = N$, (16) reduces to ${}_1F_1(N; N_R; \sigma) = \sum_{n=0}^{\infty} \frac{\sigma^n}{n!} = e^\sigma$. On the other hand, for $N_R > N$, the confluent hypergeometric function has the integral form [10, Eq. (13.4.1), p. 326] [10, Eq. (13.6.1), p. 327]

$${}_1F_1(N; N_R; \sigma) = \frac{\Gamma(N_R)}{\Gamma(N)\Gamma(N_R - N)} \int_0^1 e^{\sigma y} y^{N-1} (1-y)^{N_R-N-1} dy, \quad N_R > N, \quad (82)$$

which yields its well known infinite-series form (16), by way of the Maclaurin expansion of $e^{\sigma y}$ around $\sigma_0 = 0$, as follows [10, Eq. (13.2.4), p. 322] [10, Eq. (13.4.1), p. 326] [30, Eq. (3.191.3), p. 315] [30, Eq. (8.384.1), p. 909]:

$$\begin{aligned} {}_1F_1(N; N_R; \sigma) &= \frac{\Gamma(N_R)}{\Gamma(N)\Gamma(N_R - N)} \int_0^1 \sum_{n=0}^{\infty} \frac{\sigma^n y^n}{n!} y^{N-1} (1-y)^{N_R-N-1} dy \\ &= \frac{\Gamma(N_R)}{\Gamma(N)\Gamma(N_R - N)} \sum_{n=0}^{\infty} \frac{\sigma^n}{n!} \int_0^1 y^{n+N-1} (1-y)^{N_R-N-1} dy \\ &= \frac{\Gamma(N_R)}{\Gamma(N)\Gamma(N_R - N)} \sum_{n=0}^{\infty} \frac{\sigma^n}{n!} \frac{\Gamma(n+N)\Gamma(N_R - N)}{\Gamma(n+N_R)} \\ &= \sum_{n=0}^{\infty} \frac{\sigma^n \Gamma(n+N)\Gamma(N_R)}{n! \Gamma(N)\Gamma(n+N_R)} \\ &= \sum_{n=0}^{\infty} \frac{(N+n-1)!(N_R-1)! \sigma^n}{(N-1)!(N_R+n-1)! n!} \\ &= \sum_{n=0}^{\infty} \frac{(N)_n \sigma^n}{(N_R)_n n!} = \sum_{n=0}^{\infty} A_n(\sigma). \end{aligned} \quad (83)$$

Finally, note that ${}_1F_1(N; N_R; \sigma)$ is referred to as ‘hypergeometric’ because the ratio of two successive terms in series (83) is a rational function in n , i.e.,

$$\frac{A_n(\sigma)}{A_{n-1}(\sigma)} = \frac{N+n-1}{N_R+n-1} \frac{\sigma}{n}, \quad n \geq 1. \quad (84)$$

On the other hand, in a ‘geometric’ series, the ratio of successive terms is a constant, e.g., in $\sum_{n=0}^{\infty} \sigma^n$.

APPENDIX II

DIFFERENTIAL EQUATION W.R.T. s FOR $M(s, a)$

First, substituting σ with $\frac{as}{1-s}$ in the differential equation for ${}_1F_1(N; N_R; \sigma)$ from (28) yields

$$\frac{as}{1-s} {}_1F_1^{(2)}\left(N; N_R; \frac{as}{1-s}\right) + \left(N_R - \frac{as}{1-s}\right) {}_1F_1^{(1)}\left(N; N_R; \frac{as}{1-s}\right) - N {}_1F_1\left(N; N_R; \frac{as}{1-s}\right) = 0. \quad (85)$$

Then, from (34) we have

$$M(s, a) = \frac{1}{(1-s)^N} {}_1F_1\left(N; N_R; \frac{as}{1-s}\right), \quad (86)$$

which yields

$${}_1F_1\left(N; N_R; \frac{as}{1-s}\right) = (1-s)^N M(s, a). \quad (87)$$

Differentiating (86) w.r.t. s yields:

$$\partial_s M(s, a) = \frac{N}{(1-s)^{N+1}} {}_1F_1 \left(N; N_R; \frac{as}{1-s} \right) + \frac{a}{(1-s)^{N+2}} {}_1F_1^{(1)} \left(N; N_R; \frac{as}{1-s} \right), \quad (88)$$

By first substituting (87) into (88) and then differentiating the result w.r.t. s we obtain

$$\partial_s M(s, a) = \frac{N}{(1-s)} M(s, a) + \frac{a}{(1-s)^{N+2}} {}_1F_1^{(1)} \left(N; N_R; \frac{as}{1-s} \right), \quad (89)$$

$$\begin{aligned} \partial_s^2 M(s, a) &= \frac{N}{(1-s)^2} M(s, a) + \frac{N}{(1-s)} \partial_s M(s, a) \\ &+ \frac{a(N+2)}{(1-s)^{N+3}} {}_1F_1^{(1)} \left(N; N_R; \frac{as}{1-s} \right) + \frac{a^2}{(1-s)^{N+4}} {}_1F_1^{(2)} \left(N; N_R; \frac{as}{1-s} \right) \end{aligned} \quad (90)$$

which yield, respectively:

$${}_1F_1^{(1)} \left(N; N_R; \frac{as}{1-s} \right) = \frac{(1-s)^{N+2}}{a} \left[\partial_s - \frac{N}{(1-s)} \right] M(s, a), \quad (91)$$

$$\begin{aligned} {}_1F_1^{(2)} \left(N; N_R; \frac{as}{1-s} \right) &= \frac{(1-s)^{N+4}}{a^2} \left[\partial_s^2 M(s, a) - \frac{N}{(1-s)^2} M(s, a) \right. \\ &\quad \left. - \frac{N}{(1-s)} \partial_s M(s, a) - \frac{a(N+2)}{(1-s)^{N+3}} {}_1F_1^{(1)} \left(N; N_R; \frac{as}{1-s} \right) \right]. \end{aligned} \quad (92)$$

Substituting (91) into (92) yields:

$${}_1F_1^{(2)} \left(N; N_R; \frac{as}{1-s} \right) = \frac{(1-s)^{N+4}}{a^2} \left[\partial_s^2 - \frac{2(N+1)}{(1-s)} \partial_s + \frac{N(N+1)}{(1-s)^2} \right] M(s, a). \quad (93)$$

Finally, substituting (87), (91), and (93) into the differential equation (85), and further manipulation, yield the following differential equation w.r.t. s for $M(s, a)$

$$(s(1-s)^2 \partial_s^2 - [2(N+1)s(1-s) - (1-s)N_R + as] \partial_s + N[(N+1)s - N_R - a]) M(s, a) = 0, \quad (94)$$

which appears in the main text in (35).

APPENDIX III

INFINITE-SERIES EXPRESSIONS OF DERIVATIVES OF $p(t, a)$ W.R.T. t

Based on (18) and (33), let us define the function

$$f(t, a) = p(t, a)e^t = \sum_{n=0}^{\infty} A_n(a) \sum_{m=0}^n \binom{n}{m} (-1)^m \frac{t^{N+n-m-1}}{(N+n-m-1)!}, \quad (95)$$

whose first two derivatives are given by

$$f^{(1)}(t, a) = p^{(1)}(t, a)e^t + p(t, a)e^t, \quad (96)$$

$$f^{(2)}(t, a) = p^{(2)}(t, a)e^t + 2p^{(1)}(t, a)e^t + p(t, a)e^t. \quad (97)$$

The above yield

$$p(t, a) = f(t, a)e^{-t}, \quad (98)$$

and

$$p^{(1)}(t, a) = [f^{(1)}(t, a) - f(t, a)] e^{-t}, \quad (99)$$

$$p^{(2)}(t, a) = [f^{(2)}(t, a) - 2f^{(1)}(t, a) + f(t, a)] e^{-t}, \quad (100)$$

TABLE I
DERIVATIVES OF $f(t, a)$ FOR $N = 1, 2$

	$N = 1$	$N = 2$
$f(t, a)$	$g(t, a)$	$tg(t, a)$
$f^{(1)}(t, a)$	$g^{(1)}(t, a)$	$g(t, a) + tg^{(1)}(t, a)$
$f^{(2)}(t, a)$	$g^{(2)}(t, a)$	$2g^{(1)}(t, a) + tg^{(2)}(t, a)$

which are the only derivatives of $p(t, a)$ required for (47).

Now, if we rewrite $f(t, a)$ from (95) further as

$$f(t, a) = t^{N-1} \underbrace{\sum_{n=0}^{\infty} A_n(a) \sum_{m=0}^n \binom{n}{m} (-1)^m \frac{t^{n-m}}{(N-1+n-m)!}}_{g(t, a)} = t^{N-1} g(t, a), \quad (101)$$

then its q th derivative can be written, using Leibniz's formula [10, Eq. (1.4.12), p. 5], as

$$f^{(q)}(t, a) = \frac{d^q [t^{N-1} g(t, a)]}{dt^q} \quad (102)$$

$$= \sum_{k=0}^q \binom{q}{k} [t^{N-1}]^{(k)} g^{(q-k)}(t, a) \quad (103)$$

$$= \sum_{k=0}^q \binom{q}{k} \frac{(N-1)!}{(N-1-k)!} t^{N-1-k} g^{(q-k)}(t, a), \quad k \leq N-1. \quad (104)$$

Now, if we rewrite $g(t, a)$ as

$$g(t, a) = \sum_{n=0}^{\infty} A_n(a) \sum_{r=0}^n \binom{n}{n-r} (-1)^{n-r} \frac{t^r}{(N-1+r)!},$$

its derivative of order $q \geq 1$ is given by

$$g^{(q)}(t, a) = \sum_{n=q}^{\infty} A_n(a) \sum_{r=q}^n \binom{n}{n-r} (-1)^{n-r} \frac{1}{(N-1+r)!} \frac{r!}{(r-q)!} t^{r-q}, \quad (105)$$

On the other hand, note that going from (103) to (104) is allowed only for $k \leq N-1$. Because $k \leq q$, the requirement is that $N-1 \geq q$. Finally, because (47) requires the derivatives $f^{(q)}(t, a)$ only for $q \leq 2$, $f^{(q)}(t, a)$ can be written as in (104) only if $N \geq 3$. The remaining cases are characterized separately in Table I.

APPENDIX IV

RELATIONSHIP BETWEEN DERIVATIVES OF $M(s, a)$ W.R.T. a AND s

Differentiating (86) w.r.t. a yields

$$\partial_a M(s, a) = \frac{s}{(1-s)^{N+1}} {}_1F_1^{(1)} \left(N; N_R; \frac{as}{1-s} \right), \quad (106)$$

so that

$${}_1F_1^{(1)} \left(N; N_R; \frac{as}{1-s} \right) = \frac{(1-s)^{N+1}}{s} \partial_a M(s, a). \quad (107)$$

Now, by substituting (87) and (107) into (88), and by further manipulation, we obtain

$$a \partial_a M(s, a) = s(1-s) \partial_s M(s, a) - NsM(s, a), \quad (108)$$

which appears in the main text in (55).

REFERENCES

- [1] A. J. Paulraj, D. A. Gore, R. U. Nabar, and H. Bolcskei, "An overview of MIMO communications—A key to gigabit wireless," *Proc. of the IEEE*, vol. 92, no. 2, pp. 198–218, February 2004.
- [2] D. Gesbert, M. Kountouris, R. W. Heath, C.-B. Chae, and T. Salzer, "Shifting the MIMO paradigm," *IEEE Signal Processing Magazine*, vol. 24, no. 5, pp. 36–46, 2007.
- [3] J. Hoydis, S. ten Brink, and M. Debbah, "Massive MIMO in the UL/DL of cellular networks: How many antennas do we need?" *IEEE Journal on Selected Areas in Communications*, vol. 31, no. 2, pp. 160–171, 2013.
- [4] P. Kyosti, J. Meinila, L. Hentila, and *et al.*, "WINNER II Channel Models. Part I," CEC, Tech. Rep. IST-4-027756, 2008.
- [5] M. McKay and I. Collings, "Statistical properties of complex noncentral Wishart matrices and MIMO capacity," in *International Symposium on Information Theory, (ISIT'05)*, Sept. 2005, pp. 785 – 789.
- [6] C. Siriteanu, S. D. Blostein, A. Takemura, H. Shin, S. Yousefi, and S. Kuriki, "Exact MIMO zero-forcing detection analysis for transmit-correlated Rician fading," *IEEE Transactions on Wireless Communications*, *accepted*, December 2013. [Online]. Available: <http://arxiv.org/abs/1307.2958>
- [7] M. Jung, Y. Kim, J. Lee, and S. Choi, "Optimal number of users in zero-forcing based multiuser MIMO systems with large number of antennas," *Journal of Communications and Networks*, vol. 15, no. 4, pp. 362–369, 2013.
- [8] M. Matthaiou, C. Zhong, M. McKay, and T. Ratnarajah, "Sum rate analysis of ZF receivers in distributed MIMO systems," *IEEE Journal on Selected Areas in Communications*, vol. 31, no. 2, pp. 180–191, 2013.
- [9] C. Siriteanu, A. Takemura, S. D. Blostein, S. Kuriki, and H. Shin, "Convergence analysis of performance-measure expressions for MIMO ZF under Rician fading," in *Australian Communications Theory Workshop, (AUSCTW'14), Sydney, Australia*, Feb. 2014.
- [10] F. W. J. Olver, D. W. Lozier, R. F. Boisvert, and C. W. Clark, Eds., *NIST Handbook of Mathematical Functions*. Cambridge University Press, 2010.
- [11] K. E. Muller, "Computing the confluent hypergeometric function, $M(a, b, x)$," *Numerische Mathematik*, vol. 90, no. 1, pp. 179–196, 2001.
- [12] D. Zeilberger, "A holonomic systems approach to special functions identities," *Journal of computational and applied mathematics*, vol. 32, no. 3, pp. 321–368, 1990.
- [13] C. Mallinger, "Algorithmic manipulations and transformations of univariate holonomic functions and sequences," Ph.D. dissertation, Johannes Kepler University Linz, Austria, 1996.
- [14] M. Kauers and P. Paule, *The Concrete Tetrahedron: Symbolic Sums, Recurrence Equations, Generating Functions, Asymptotic Estimates*. Springer Wien, 2011.
- [15] T. Hibi, Ed., *Groebner Bases. Statistics and Software Systems*. Tokyo, Japan: Springer, 2013.
- [16] T. Sei and A. Kume, "Calculating the normalising constant of the Bingham distribution on the sphere using the holonomic gradient method," *Statistics and Computing*, pp. 1–12, 2013.
- [17] H. Hashiguchi, Y. Numata, N. Takayama, and A. Takemura, "The holonomic gradient method for the distribution function of the largest root of a Wishart matrix," *Journal of Multivariate Analysis*, vol. 117, pp. 296–312, 2013.
- [18] M. K. Simon and M.-S. Alouini, *Digital Communication Over Fading Channels. A Unified Approach to Performance Analysis*. Baltimore, Maryland: John Wiley and Sons, 2000.
- [19] S. Loyka and G. Levin, "On physically-based normalization of MIMO channel matrices," *IEEE Transactions on Wireless Communications*, vol. 8, no. 3, pp. 1107–1112, March 2009.
- [20] D. A. Gore, R. W. Heath Jr, and A. J. Paulraj, "Transmit selection in spatial multiplexing systems," *IEEE Communications Letters*, vol. 6, no. 11, pp. 491–493, 2002.
- [21] M. Kiessling and J. Speidel, "Analytical performance of MIMO zero-forcing receivers in correlated Rayleigh fading environments," in *IEEE Workshop on Signal Processing Advances in Wireless Communications (SPAWC'03)*, June 2003, pp. 383–387.
- [22] C. Siriteanu, Y. Miyayama, S. D. Blostein, S. Kuriki, and X. Shi, "MIMO zero-forcing detection analysis for correlated and estimated Rician fading," *IEEE Transactions on Vehicular Technology*, vol. 61, no. 7, pp. 3087–3099, September 2012.
- [23] M. Saito, B. Sturmfels, and N. Takayama, *Gröbner Deformations of Hypergeometric Differential Equations*, ser. Algorithms and Computation in Mathematics. Springer, 2011.
- [24] J. G. Proakis, *Digital Communications*, 4th ed. New York, NY: McGraw-Hill, Inc., 2001.
- [25] P. Koev and A. Edelman, "The efficient evaluation of the hypergeometric function of a matrix argument," *Mathematics of Computation*, vol. 75, no. 254, pp. 833–846, 2006.
- [26] A. J. Grant, "Performance analysis of transmit beamforming," *IEEE Transactions on Communications*, vol. 53, no. 4, pp. 738–744, 2005.
- [27] R. J. Muirhead, "Systems of partial differential equations for hypergeometric functions of matrix argument," *The Annals of Mathematical Statistics*, vol. 41, no. 3, pp. 991–1001, 1970.
- [28] I. G. Macdonald, "Hypergeometric functions I," *arXiv preprint arXiv:1309.4568*, 2013. [Online]. Available: <http://arxiv.org/abs/1309.4568>
- [29] C. Koutschan. HolonomicFunctions package for Mathematica. Research Institute for Symbolic Computation (RISC). Johannes Kepler University, Linz, Austria. [Online]. Available: <http://www.risc.jku.at/research/combinat/software/ergosum/RISC/HolonomicFunctions.html>
- [30] I. S. Gradshteyn and I. M. Ryzhik, *Table of Integrals, Series, and Products*, 7th ed. Elsevier, Academic Press, 2007.